Use of the steric mass action model in ion-exchange chromatographic process development[1]

Harish Iyer*, Sarah Tapper[2], Philip Lester, Bradley Wolk, Robert van Reis

Department of Recovery Sciences, Genentech Inc., 1 DNA Way, S. San Francisco, CA 94080 USA

Abstract

Despite the preponderance of models in the literature, chromatographic process development in industrial protein purification has traditionally been based on heuristic knowledge and expertise. In this work, we explore the feasibility of using a mathematical model to guide process development and optimization. The development of an anion-exchange step to separate an antibody from its dimer is used as a paradigm to test this approach to process development. In the approach involving models, we show that the work required may be reduced to the task of determining conditions for adequate selectivity. Once these conditions are obtained, the steric mass action formalism is used to predict the preparative experimental results. Our results indicate that this model is able to accurately predict experimental results under high loadings with minimal parameter estimation. Finally, we identify ways in which such models can be used to increase productivity and process robustness. © 1999 Elsevier Science B.V. All rights reserved.

Keywords: Steric mass action model; Optimization; Mathematical modelling; Proteins

1. Introduction

Traditionally, chromatographic process development for protein purification has been based on heuristic knowledge and expertise. In this work, we show that a simple model can be a useful tool in aiding traditional process development efforts and understanding the performance of a chromatographic step. Apart from aiding process development, this approach also has the potential to improve the understanding of the robustness of a step (sensitivity to process conditions), determining rational ranges for manufacturing operation (process validation) and troubleshooting process variation at full scale.

While there have been extensive contributions from academia on modelling preparative chromatography of proteins, there have been relatively few attempts at using models for industrial mixtures. Yamamoto and co-workers [1,2] have employed a continuous-flow plate model in conjunction with a linear isotherm to characterize and scale up gradient operations. They have employed these methods to

scale up β-galactosidase purification in a 30 l column based upon data obtained with a 23 ml column [3]. Recently, Feng and Watler [4] have used Yamamoto's approach to determine scale-up of a linear gradient in their recovery process [4]. On the other hand, Johnson and Frenz [5] have used a multi-component Temkin isotherm to model the fractionation of a heterogeneous mixture of a variably glycosylated protein. Recently, Shukla et al. [6] have used selective displacement chromatography for the purification of an antigenic protein from an industrial process stream. In their work, the steric mass action (SMA) formalism was utilized to construct an operating regime plot [7] and thus, establish appropriate conditions for selective displacement chromatography.

The SMA model describes protein adsorption in ion-exchange systems as a stoichiometric exchange [8]. At higher protein concentrations, the finite capacity of the stationary phase and the steric shielding of stationary phase sites [9] by the adsorbed molecules play important roles in equilibrium adsorption. Velayudhan [10] observed that the number of blocked sites is proportional to the adsorbed protein concentration. Brooks and Cramer [11] have utilized this insight to form the basis of the SMA formalism. The SMA model has been shown capable of describing the linear and nonlinear adsorption of proteins in ion-exchange chromatographic systems over a range of salt concentrations [12]. Further, it has been shown to accurately predict the nonlinear behavior of multicomponent protein adsorption in isocratic [13], step gradient [14], linear gradient [15] and displacement modes [12] using model protein mixtures. A comparison of the SMA model (see Appendix A for a summary of the model equations) with other models in the literature is presented in Table 1.

In this paper, the SMA model was employed to investigate the utility of mathematical models in chromatographic process development. The chromatographic process involved the preparative separation of a recombinant antibody from its dimer using anion-exchange chromatography. A case study approach was used to study the ability of the model to predict separations over a wide range of process parameters.

2. Theory

2.1. Model

The SMA model has been described previously in the chromatographic literature [11]. The key parameters of the model are shown in Table 2. The linear model parameters, which are the characteristic charge, ν_i and the equilibrium binding constant, K_i, define the retention time of a protein pulse under dilute conditions at a given salt concentration, and are used to determine the time of protein elution from a column. The steric factor, σ, along with the ionic capacity, Λ, is reflective of the maximum capacity of the protein and is used to describe the nonlinear adsorption behavior. All of the model parameters combine to give a description of the partitioning of the protein between the stationary and mobile phases at a given pH and in a specific buffer at various salt concentrations.

3. Materials and methods

3.1. Materials used in preparative chromatography experiments

Q-Sepharose FF resin (Lot No. 241507, QSFF)

Table 1
Some isotherms and the different facets of protein adsorption that they can describe

Isotherm type	Linear adsorption	Nonlinear adsorption	Salt ion dependence of isotherm	Induced salt gradients
Henry's Law [16]	Yes	No	No	No
Langmuir [17]	Yes	Yes	No	No
Freundlich [18]	No	Yes	No	No
Temkin [19]	Yes	Yes	No	No
Modifier-dependent Langmuir [20]	Yes	Yes	Yes	No
SMA [21]	Yes	Yes	Yes	Yes

Table 2
SMA model parameters and their putative interpretation

Parameter symbol (units)	Parameter name	Interpretation of parameter
ν (–)	Characteristic charge	The number of sites that the protein interacts with on the resin surface
K (–)	Binding constant	The binding constant for the stoichiometric binding reaction between the protein and the salt counterions
Λ (mM)	Ionic or bed capacity	The total number of binding sites available on the resin surface in mmol per liter stationary phase
σ (–)	Steric factor	The number of sites on the surface that are shielded by the protein and prevented from exchange with the salt counterions in solution

was obtained from Pharmacia (Piscataway, NJ, USA). A 6.2-ml (6.6 cm×1.1 cm diameter) column obtained from Omni was packed with the QSFF resin. Buffers were prepared by dilution of stock solutions (Media Prep facility, Genentech, South San Francisco, CA, USA) using purified water. Protein load containing antibody monomer (M_r 150 000) and dimer (M_r 300 000) was obtained from Manufacturing at Genentech. The protein solution was diluted with purified water to attain a final conductivity of approximately 4 mS/cm. A calculated volume of 1 M Tris–HCl, pH 8 solution was also added to condition the protein solution to 25 mM Tris, pH 8. The addition of water and the pH adjustment were used to enable the protein to bind to the QSFF column during loading in the preparative experiments. The final concentrations of monomer and dimer in the load were 3.14 mg/ml and 0.25 mg/ml, respectively. All preparative experiments were done using either a Biosys 2000 (Beckman Instruments, Fullerton, CA, USA) or an Åkta Explorer (Pharmacia).

3.2. Porosity measurement

The total porosity (interstitial and intraparticle) of the packed column was determined by injecting a 50-μl pulse of 0.2 M sodium nitrate (salt obtained from Sigma, St. Louis, MO, USA) through the Biosys chromatographic system both in the presence and absence of the column. The system dead volume is obtained in the absence of the column. The residence time in the presence of the column and the empty column volume are used to obtain the total porosity of the packed volume. Detection of sodium

nitrate was achieved by monitoring UV absorbance at 280 nm at the column outlet.

3.3. Fraction analysis in preparative experiments

Fractions collected during preparative chromatography experiments were analyzed using high-performance size-exclusion chromatography (HPSEC) on a HP1050 analytical chromatography system (Hewlett-Packard, Mountain View, CA, USA). A Superdex 200 HR 10/30 column (Pharmacia) was run isocratically at 1 ml/min with phosphate buffered saline [composition: NaCl (8.0 g/l), KCl (0.2 g/l), Na_2HPO_4 (1.13 g/l), KH_2PO_4 (0.2 g/l), pH 7.2] as the running buffer. Antibody monomer and dimer concentrations were determined via online UV detection at 214 nm.

3.4. Model linear parameters

The ionic capacity of the resin, Λ, was obtained from a certificate of analysis from Pharmacia for the specified lot. The linear parameters ν_i and K_i have traditionally been determined from retention times obtained from isocratic experiments [11]. In the isocratic experiments that were carried out with the antibody monomer/dimer mixture, the retention times of the dimer peaks could not be determined because of dispersion effects. Therefore, linear gradients were used to determine these parameters. In this gradient method, the monomer and dimer peaks could be distinctly resolved and identified because of the lower dispersion in a gradient relative to an isocratic step. The antibody monomer and dimer peak positions were determined for analytical (100

μl) injections at three different gradient volumes at 1 ml/min. All the gradients were from 75 to 425 mM sodium chloride in 25 mM Tris, pH 8 buffer with gradient volumes of 20, 25 and 30 column volumes (CVs). From the peak positions of the antibody monomer and dimer in these three gradients, unique values of ν_i and K_i were determined by using the methodology of Parente and Wetlaufer [22].

3.5. Model nonlinear parameters and computational grid size

In order to simulate SMA chromatograms, two additional parameters are required. The first parameter is the steric factor, σ, which describes the nonlinear chromatographic behavior of the protein on the resin [11]. The second parameter is the size of the grid used (Δz) in the numerical solution to the equations. The choice of the grid size in the computational solution to the SMA equations directly impacts the simulated dispersion of the protein peaks: coarser grids (larger Δz) cause greater dispersion and spreading. In the absence of a second-order dispersion term in the transport equations, the experimentally observed dispersion has to be simulated by manipulating the grid size. Note that in order to maintain computational stability, Δt chosen to be less than Δz by setting $\Delta t = 0.95 \Delta z$. In this paper, both the steric factor and the grid dimensions were obtained from a least-squares fit to an experimental chromatogram. In obtaining the experimental chromatogram for this fit, the antibody monomer and

dimer were initially loaded on to the column at 30 mg of total protein per ml of resin. The protein was then eluted in a 45 CV salt gradient from 50 mM to 500 mM NaCl in a 25 mM Tris, pH 8 background. Two-ml fractions were collected when the protein began to break through and were analyzed using HPSEC to construct the chromatographic profile.

3.6. Preparative experiments to test SMA model

In order to test the ability of the SMA model to predict separation results, several experiments were carried out in both gradient and step elution modes. Table 3 outlines the preparative gradient experiments. The column was initially loaded with a specific mass of protein per liter of resin. The protein was then immediately eluted with a specified gradient. The gradient conditions chosen span a wide range of important parameters such as gradient volume (5–45 CVs), protein loading (5 to 30 mg of protein per ml of resin), and initial and final NaCl concentrations in the gradient. In the step elution experiments, the resin was initially loaded with 20 g of protein per liter of resin. Following the load, step elutions at 25 mM Tris, pH 8 and a specified NaCl concentration were carried out. In all, seven different step elution experiments were carried out at NaCl concentrations of 100, 120, 140, 150, 160, 180 and 200 mM. In both the gradient and step elution experiments, 2-ml fractions were collected from the beginning of the elution step. These fractions were analyzed for antibody monomer and dimer concen-

Table 3
Preparative gradient experiments using antibody monomer and dimer on Q-Sepharose FF

	Gradient volume (CV)	Loading (mg/ml)	Initial NaCl concentration (mM)	Final NaCl concentration (mM)
1	45	30	50	400
2	45	24	50	400
3	10	10	25	200
4	10	20	25	200
5	5	5	25	200
6	5	5	75	200

Initial protein concentration: 3.4 mg/ml: 7.5% dimer (0.25 mg/ml dimer + 3.14 mg/ml monomer); bed volume: 6.2 ml; initial and final gradient salt: NaCl as specified and 25 mM Tris at pH 8; velocity: 20 CV/h.

trations using HPSEC. Based on the data from the analyzed fractions, yields of antibody monomer were computed at the process goal of 99% pure monomer. These yields were then compared to yields obtained from simulations using the SMA isotherm in concert with an equilibrium dispersive model [14].

3.7. SMA model simulations

The numerical solution to the SMA model coupled with the equilibrium-dispersive model equations for the specified load and elution conditions was determined using a Fortran code [14]. Model simulations were carried out on a Compaq DeskPro 5133 Personal Computer using a Fortran Visual Workbench v1.00 compiler (Microsoft). Dispersion of the proteins was simulated by manipulating computational grid size [14]. The results of the SMA simulation are in the form of chromatograms. Yields and purities of the desired product can be computed at various points along the simulated model chromatogram.

4. Results and discussion

4.1. Model parameters

The porosity of the resin was determined to be 0.695 based on pulse experiments in the presence and absence of the column. The ionic capacity of the resin, Λ, was obtained as 200 mM from the certificate of analysis for the resin lot. The model linear parameters ν_i and K_i were then calculated from least-squares fits to peak positions obtained from gradient elutions of analytical injections (method outlined in Refs. [22,23]). The nonlinear parameter, σ, for the antibody monomer, was determined from a model fit to the initial preparative experiment with a 45-CV gradient. The goodness of the fit was determined by a least-squares comparison of the experimental data and the model simulation.

Both the steric factor, σ, and the numerical grid size were simultaneously fit using a least-squares fit to the experimental chromatogram in Fig. 1. The value of the monomer σ was 80. The profile of the dimer was insensitive to different values of the
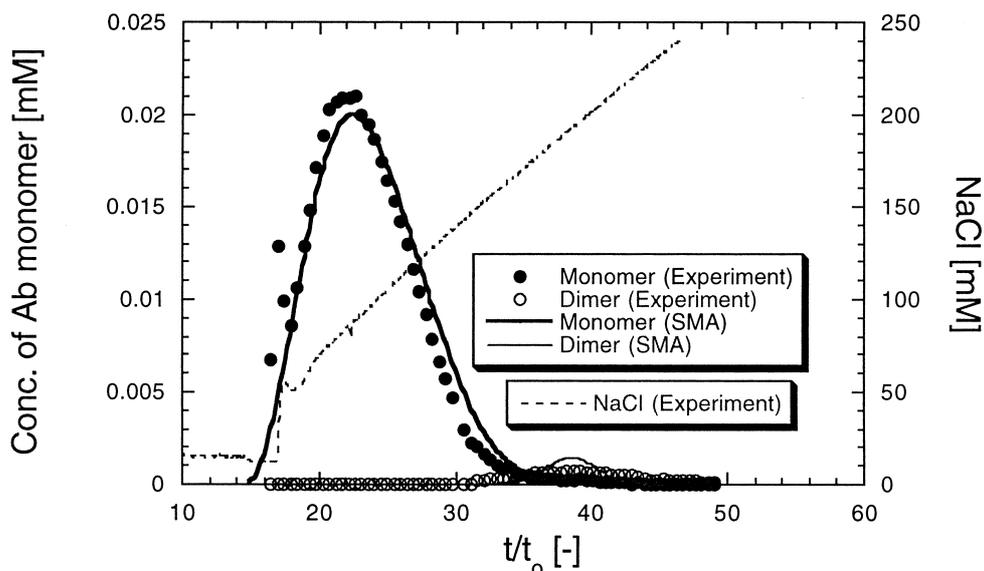

Fig. 1. Comparison of experimental and simulated chromatograms for antibody monomer/dimer separation on Q-Sepharose FF. Experimental conditions: 24 mg/ml load, 45-CV gradient from 50 mM NaCl to 400 mM NaCl, 20 CV/h, 6.2 ml column. CV stands for column volume.

nonlinear SMA parameter, σ. This is presumably because the dimer concentrations observed are in the linear region of the dimer isotherm. The best fit value for Δz was obtained as 0.5. The temporal grid size was $\Delta t = 0.95\Delta z$. These grid dimensions were then kept constant in the rest of the gradient and step elution simulations. The values of all the final model parameters are shown in Table 4.

4.2. Use of SMA model to predict preparative chromatographic behavior

Several simulated gradient and step elution separations of the antibody monomer/dimer mixture were carried out on the computer using the SMA model. At the same time, separation experiments were also carried out under the same conditions. A comparison of a simulated and an experimental chromatogram from a gradient purification experiment is shown in Fig. 1. This figure shows good agreement between the simulated curve and the experimental data points for the monomer profile and fair agreement for the dimer. The dimer profile is also broader than predicted; this is not due to protein heterogeneity (data not shown), but could be due to larger dispersive effects as compared to the monomer. The yields of antibody monomer can be computed at a specified purity from such chromatograms. Fig. 2 shows the yields of antibody monomer at 99% purity from all the gradient experiments. Also plotted on the figures are predictions of yields (at 99% purity) based on SMA model simulations. The simulation results and the experimental data are in good agreement. Consider the first two SMA simulation points in Fig. 2. The model indicates that an increase in the initial salt concentration from 25 mM NaCl to 75 mM NaCl results in an increase in the

yield. This increase in yield is not intuitive; it is the net result of the changed selectivities of the antibody monomer and dimer molecules at the various salt concentrations along this new gradient. The experimental data match this increase in yield indicating the power of such model predictions. It is, however, important to note that the model overpredicts the yield to a certain extent because it does not capture the dispersion of the dimer completely. Finally, the last four model simulation points in Fig. 2 are most relevant as they indicate 100% recovery of monomer. The corresponding experimental yields range from 96% to 98.5%. The errors in the model are small considering the range of process parameters used in these simulations. Also, the model narrows the process parameter space and helps to identify a smaller set of final gradient experiments.

The results of SMA simulations and step elution experiments are shown in Fig. 3. The general trend shown in the simulations is tracked by the experimental results. Again, using easily measured parameters, the model is able to identify various regimes in which process development could be pursued. For example, simulations indicate that step elution at salt concentrations between 100 mM NaCl and 140 mM NaCl could separate the monomer and dimer with a high yield. From Fig. 3, it can also be seen that in the range of 140–170 mM NaCl, the model is able to identify "cliffs" or "edges-of-failure" where small changes in salt concentration could cause precipitous drops in yield. This knowledge enables a better understanding of the robustness of such step elutions. Comparing results in the salt range of 140–170 mM, one notices differences between model and experiment. These differences between observed and model predictions are again primarily attributable to the simplicity with which dispersion has been modeled here. While the true dispersion of the monomer and dimer are both simulated here using numerical grid-based dispersion [24,25], a more sophisticated treatment [26] may bring the model and experimental data in closer agreement.

Table 4
SMA model parameters ($\Lambda = 200$ mM, porosity, $\epsilon = 0.695$)

Species	ν	K	σ
Antibody monomer	4.02 ± 0.02	2.53 ± 0.03	80
Antibody dimer	14.28 ± 0.13	8.60 ± 0.14	150[a]

Standard deviations in the SMA linear parameters are based on estimated errors in retention times of ± 0.1 min.
[a] The simulated dimer chromatogram is insensitive to the value of σ. A value of 150 was used in order to carry out model simulations.

5. Conclusions

The SMA model has been used to predict yield in

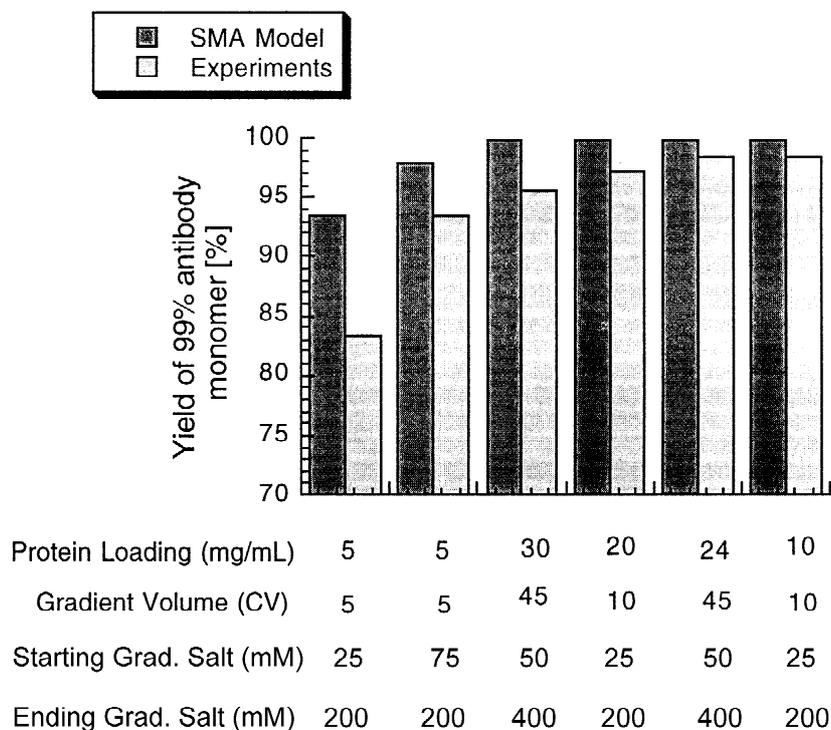| Protein Loading (mg/mL) | 5 | 5 | 30 | 20 | 24 | 10 |
Gradient Volume (CV)	5	5	45	10	45	10
Starting Grad. Salt (mM)	25	75	50	25	50	25
Ending Grad. Salt (mM)	200	200	400	200	400	200

Fig. 2. Yield of antibody monomer (at 99% purity) from different gradient experiments and the corresponding SMA model simulation results. Protein loading (mg/ml of resin), gradient volume in CVs, salt concentrations at start and end of gradient are specified. The flow-rates were all 20 CV/h (2.1 ml/min). CV stands for column volume.
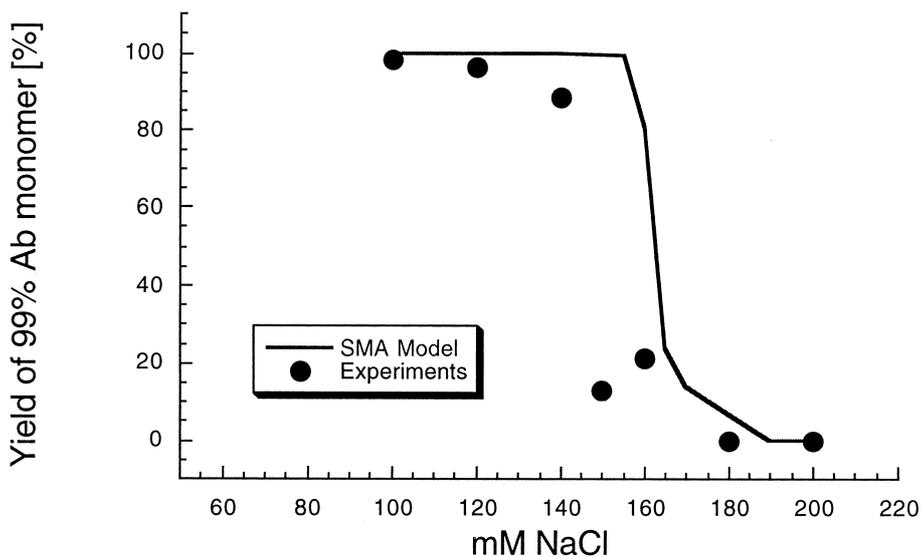

Fig. 3. Yield of antibody monomer (at 99% purity) from different step elution experiments and the corresponding SMA model simulations. Loading in all these experiments was 20 mg of protein per ml of resin. In addition to NaCl, the elution buffer contained 25 mM Tris–HCl and was at pH 8. The flow-rate in all these experiments was 20 CV/h. CV stands for column volume.

both gradient and step elution separations in the anion-exchange chromatography of antibody monomer and dimer. The model employed three independently obtained parameters (ν, K and Λ) and one fitted parameter (σ). Predicted model yields were matched fairly well by the experimental results. Both the model and experimental results indicate that either step or gradient elutions could separate antibody dimer from monomer. The final choice of the process to be used in manufacturing is still left up to the process development team with other considerations such as accuracy of buffer makeup, validation of endotoxin, virus and DNA removal, tankage in the plant and robustness of gradient operation.

As shown in this work, the model allows for a more rigorous approach to process development with fewer laboratory experiments than a heuristic approach. In this study, the model parameters were measured within a period of two to three days. Following this, all the gradient and step elution simulations were carried out in less than a day to define the process space in which experiments needed to be performed. This contrasts with a traditional approach where more than four weeks worth of work may be required to explore the entire process space. This shows that savings in time required for process development may be significant. The model has also been shown to be useful in determining "edges-of-failure" that are otherwise hard to determine without extensive experimental work. From the results shown here, it is clear that a model-aided approach to process development may provide insight into process performance and a crucial advantage in speeding up development of robust chromatographic processes.

There are several other benefits to the model-based approach that have not been touched upon so far. These include the ability to set rational ranges for operation of gradient, isocratic and step elution operations in manufacturing. When a resin lot is changed, remeasuring the SMA model parameters and analyzing the results of simulated separations may provide insight into potential changes in the chromatographic performance. For instance, knowing that a resin's ionic capacity was important in maintaining chromatographic selectivity could help maintain optimum performance in the plant when new raw materials are introduced.

There are however, limitations to situations in which this approach may help process development. First, it is most valid when there are relatively few quantifiable components in protein loads (trace impurities, such as DNA and host cell proteins, are harder to quantify and characterize due to their heterogeneity and their propensity to disperse in a gradient). Second, this model would have to be modified to account for heterogeneity in the protein population due to variable glycosylation which disperses peaks significantly under isocratic conditions. Third, unless the parameters are independently measured at the different pH and buffer salts, one cannot extrapolate results across pH and buffer salts.

6. Symbols

ϵ (–)	Porosity of the column=pore volume/column volume
σ_i (–)	Steric factor of species i
ν_i (–)	Characteristic charge of species i
Λ (mM)	Ionic capacity of the resin
$K_{1,i}$ (–)	Equilibrium constant for ion-exchange process
C_i (mM, mg/ml)	Concentration of protein i in the mobile phase
$C_{fi,\ eed}$ (mM, mg/ml)	Concentration of protein i in the feed
G_{fslope} (mM)	Dimensionless gradient slope $=[(C_{salt,\ final}-C_{salt,\ initial})/$ (No. of column volumes)$\cdot\epsilon]$
L (cm)	Column length
Q_i (mM, mg/ml)	Concentration of protein i on the stationary phase
Q_i^* (mM, mg/ml)	Equilibrium concentration of protein i on the stationary phase
t (–)	Dimensionless time$=t/t_0$
t_0	Column residence time for unretained solute=[(column volume$\cdot\epsilon$)/(flow-rate)
t_{feed} (–)	Dimensionless time for protein feed=[(Load volume)/ (Column volume$\cdot\epsilon$)]
z (–)	Dimensionless axial column length

Acknowledgements

We would like to gratefully acknowledge the contributions of Professor Steven Cramer, Dr. Kris Barnthouse and Mr. Venkatesh Natarajan to this manuscript.

Appendix A

Summary of the SMA model

The exchange of counterions and the protein in the SMA model is represented by the following stoichiometric equation

$$C_i + \nu_i \bar{Q}_1 \overset{K_{1,i}}{\leftrightarrow} Q_i + \nu_i C_1 \tag{A1}$$

The mass balance for the sites on the bed and the equilibrium relationship between the counterions and the protein are given by Eqs. (A2) and (A3), respectively.

$$\Lambda = \bar{Q}_1 + \sum_{i>1}(\nu + \sigma)Q_i \tag{A2}$$

$$K_1 = \left(\frac{Q_i}{C_i}\right)\left(\frac{C_1}{\bar{Q}_1}\right)^{\nu_i} \tag{A3}$$

Table 2 illustrates the significance of the parameters in Eqs. (A2) and (A3).

To carry out the SMA model simulation, Eqs. (A1)–(A3) are solved in conjunction with the transport equation

$$\beta\frac{\partial Q_i}{\partial t} + \frac{\partial C_i}{\partial z} + \frac{\partial C_i}{\partial t} = 0, \; i = 1, \ldots, \text{NC} \tag{A4}$$

where z is the axial column length nondimensionalized by column length L, and t is time nondimensionalized by the column residence time t_0 and NC is the total number of components. In linear gradient chromatography, the salt (component 1) concentration is a ramp function at the column inlet:

$$\begin{aligned} C_1(t \le t_{\text{feed}}, 0) &= C_{1,\text{ feed}} \\ C_1(t > t_{\text{feed}}, 0) &= C_{1,\text{f}} + \left[G_{\text{slope}}(t - t_{\text{feed}})\right] \end{aligned} \tag{A5}$$

where t_{feed} is the duration of the feed pulse and G_{slope} is the dimensionless gradient slope. For both the antibody monomer (component 2) and dimer (component 3), the initial and boundary conditions are

$$\begin{aligned} C_2(t < 0, 0) &= 0 \\ C_2(0 < t < t_{\text{feed}}) &= C_{\text{monomer, feed}} \\ C_2(t > t_{\text{feed}}, 0) &= 0 \; (\text{Elution}) \end{aligned}$$

$$\begin{aligned} & \\ C_3(t < 0, 0) &= 0 \\ C_3(0 < t < t_{\text{feed}}, 0) &= C_{\text{dimer, feed}} \\ C_3(t > t_{\text{feed}}, 0) &= 0 \; (\text{Elution}) \end{aligned} \tag{A6}$$

References

[1] S. Yamamoto, K. Nakanishi, R. Matsuno, T. Kamibuko, Biotechnol. Bioeng. 25 (1983) 1465.
[2] S. Yamamoto, M. Nomura, Y. Sano, AIChE J. 33 (1987) 1426.
[3] S. Yamamoto, M. Nomura, Y. Sano, J. Chromatogr. 409 (1987) 101.
[4] D. Feng, P. Watler, Recovery of Biological Products VIII, Engineering Foundation Conference, Tuscon, AZ, 1996.
[5] R. Johnson, J. Frenz, Recovery of Biological Products VIII, Engineering Foundation Conference, Tucson, AZ, 1996.
[6] A.A. Shukla, R.L. Hopfer, E. Bortell, D. Chakrabari, S.M. Cramer, Biotechnol. Prog. 14 (1998) 92.
[7] S.R. Gallant, S.M. Cramer, J. Chromatogr. A 771 (1997) 9.
[8] N.K. Boardman, S.M. Partridge, Biochem. J. 59 (1955) 543.
[9] R.D. Whitely, R. Wachter, F. Liu, N.-H.L. Wang, J. Chromatogr. 465 (1989) 137.
[10] A. Velayudhan, Doctoral Dissertation, Yale University, New Haven, CT, 1990.
[11] C.A. Brooks, S.M. Cramer, AIChE J. 38 (1992) 1969.
[12] S.D. Gadam, G. Jayaraman, S.M. Cramer, J. Chromatogr. 630 (1993) 37.
[13] S.R. Gallant, A. Kundu, S.M. Cramer, J. Chromatogr. A 702 (1995) 125.
[14] S.R. Gallant, A. Kundu, S.M. Cramer, Biotechnol. Bioeng. 47 (1995) 125.
[15] S.R. Gallant, S. Vunnum, S.M. Cramer, J. Chromatogr. A 725 (1996) 295.
[16] L.R. Snyder, in: Cs. Horváth (Ed.), High-Performance Liquid Chromatography, Academic Press, New York, 1980, p. 280.
[17] I. Langmuir, J. Am. Chem. Soc. 38 (1916) 2221.
[18] H. Freundlich, Phys. Chem. 57 (1907) 385.
[19] M.L. Temkin, Zh. Fiz. Khim. 14 (1940) 1153.
[20] F.D. Antia, Cs. Horváth, J. Chromatogr. 484 (1989) 1.
[21] C.A. Brooks, S.M. Cramer, Chem. Eng. Sci. 51 (1996) 3847.
[22] E.S. Parente, D.B. Wetlaufer, J. Chromatogr. A 333 (1986) 29.
[23] K. Barnthouse, Doctoral dissertation, Rensselaer Polytechnic Institute, Troy, NY, 1998.
[24] M. Czok, G. Guichon, Anal. Chem. 62 (1990) 189.
[25] Z. Ma, G. Guichon, Comput. Chem. Eng. 15 (1991) 415.
[26] P. Schneider, J.M. Smith, AIChE J. 14 (1968) 762.